iScience

CellPress
OPEN ACCESS

Article

Impaired synaptic plasticity in an animal model of autism exhibiting early hippocampal GABAergic-BDNF/TrkB signaling alterations

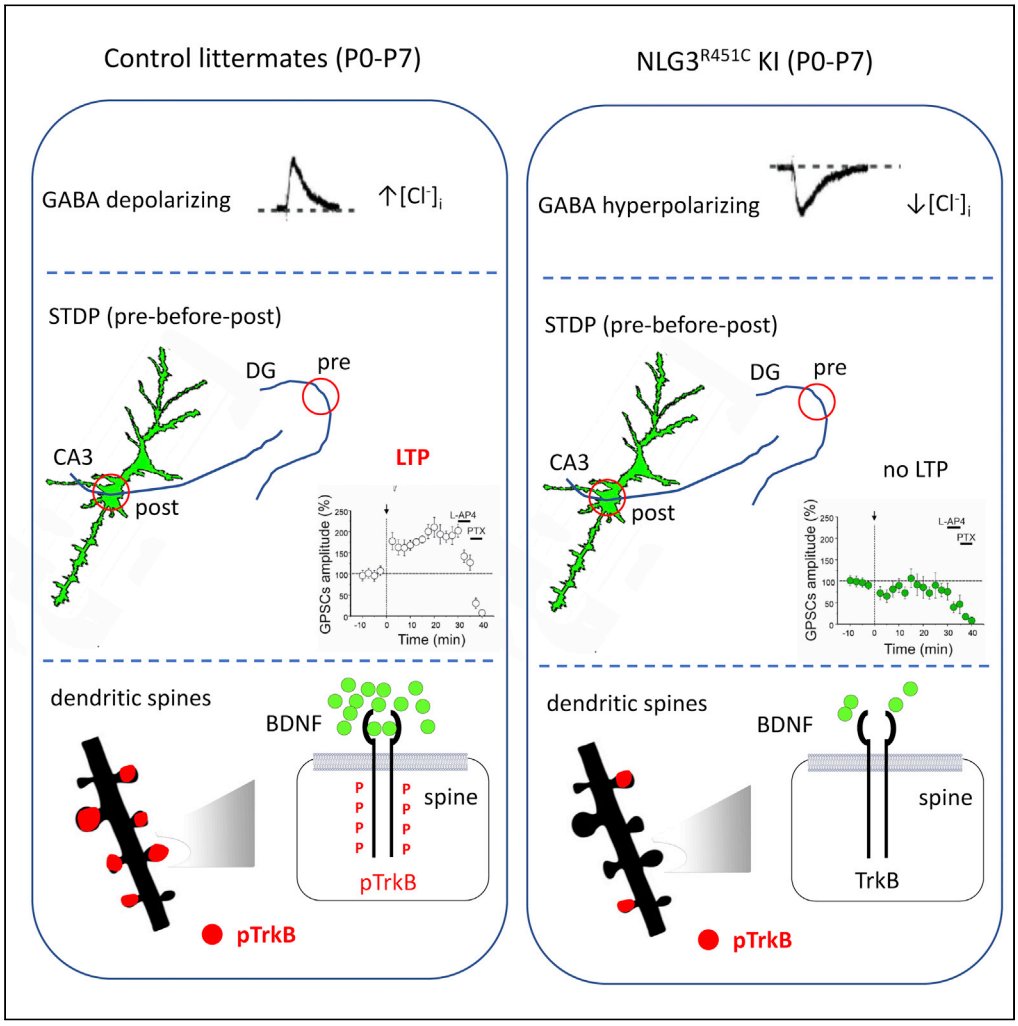

Martina Sgritta, Beatrice Vignoli, Domenico Pimpinella, ..., Cristina Marchetti, Marco Canossa, Enrico Cherubini

marco.canossa@unitn.it (M.C.)
cher@sissa.it (E.C.)

Highlights

Early hyperpolarizing action GABA at immature MF-CA3 synapses in NLG3^{R451C} KI mice

Loss of STD-LTP at mossy fibers (MF)-CA3 synapses in NLG3^{R451C} KI and NLG3 KO mice

The loss of STD-LTP persists in mutated mice at adult glutamatergic MF-CA3 synapses

Impairment of BDNF/TrkB signaling at potentiated MF-CA3 synapses of mutated mice

Sgritta et al., iScience 26, 105728
January 20, 2023
https://doi.org/10.1016/j.isci.2022.105728

iScience

CellPress
OPEN ACCESS

Article

Impaired synaptic plasticity in an animal model of autism exhibiting early hippocampal GABAergic-BDNF/TrkB signaling alterations

Martina Sgritta,[1,8] Beatrice Vignoli,[2,8] Domenico Pimpinella,[1] Marilena Griguoli,[1,3] Spartaco Santi,[4] Andrzej Bialowas,[5] Grzegorz Wiera,[5] Paola Zacchi,[6] Francesca Malerba,[1] Cristina Marchetti,[1,3] Marco Canossa,[7,*] and Enrico Cherubini[1,5,9,*]

SUMMARY

In Neurodevelopmental Disorders, alterations of synaptic plasticity may trigger structural changes in neuronal circuits involved in cognitive functions. This hypothesis was tested in mice carrying the human R451C mutation of *Nlgn3* gene (NLG3^{R451C} KI), found in some families with autistic children. To this aim, the spike time dependent plasticity (STDP) protocol was applied to immature GABAergic Mossy Fibers (MF)-CA3 connections in hippocampal slices from NLG3^{R451C} KI mice. These animals failed to exhibit STD-LTP, an effect that persisted in adulthood when these synapses became glutamatergic. Similar results were obtained in mice lacking the *Nlgn3* gene (NLG3 KO mice), suggesting a loss of function. The loss of STD-LTP was associated with a premature shift of GABA from the depolarizing to the hyperpolarizing direction, a reduced BDNF availability and TrkB phosphorylation at potentiated synapses. These effects may constitute a general mechanism underlying cognitive deficits in those forms of Autism caused by synaptic dysfunctions.

INTRODUCTION

Autism Spectrum Disorders (ASDs) are neuro-developmental disorders with a strong genetic component, characterized by deficits in verbal and non-verbal communication, impairment of social interaction, restricted interests, and stereotyped behavior. Most genes implicated in ASDs encode proteins relevant for transcriptional regulation, chromatin remodeling and synaptic function.[1–5] Among synaptic proteins, of particular interest are those implicated in scaffolding and structuring such as those belonging to the neuroligin (NLG)/neurexin (NRX) families.[5,6] NLGs are postsynaptic proteins that, by interacting with their presynaptic partners NRXs, functionally couple the postsynaptic densities with the transmitter release machinery, thus contributing to synaptic development and stabilization.[5] Mutations or deletions of *Nlgn1-4* genes,[7–9] localized mainly on human chromosome loci Xq13 and Xq22.33, are often associated with ASDs. One of these mutations, the R451C, within the highly conserved region of the extracellular esterase-homology domain of the *Nlgn3* gene, found in a family with children affected by ASDs,[7] has been introduced in mice by gene targeting techniques.[10] These mice displayed circuit- and cell-specific synaptic dysfunctions in several brain areas. In particular, NLG3^{R451C} KI, but not NLG3 KO mice, exhibited an increase of synaptic inhibition but not excitation in layer $^{2}/_{3}$ somatosensory cortex, suggesting a gain of function. These alterations were associated with deficits in social interactions.[10–17] However, in contrast to somatosensory cortex, the CA1 region of the hippocampus of NLG3^{R451C} KI exhibited an enhanced excitatory synaptic transmission associated with an up-regulation of AMPA and NMDA receptors containing the NR2B subunits, an increased number of dendritic branches in stratum radiatum and a more pronounced LTP.[12]

A more detailed analysis of neuronal circuits underlying behavioral deficits in NLG3^{R451C} KI mice, has unveiled a decreased release of GABA from parvalbumin-positive basket cells, mediating feedforward and feedback inhibition in both hippocampus[17] and somatosensory cortex.[18] This may affect the temporal precision of action potential generation[19] and the excitatory/inhibitory (E/I) balance within selective neuronal circuits. The consequent impaired coordination of distributed neuronal activity may alter

[1]European Brain Research Institute (EBRI), 00161 Rome, Italy

[2]Department of Physics, University of Trento, Povo, 38123 TN, Italy

[3]Institute of Molecular Biology and Pathology, National Research Council, 00185 Rome, Italy

[4]Institute of Molecular Genetics "Cavalli-Sforza", National Research Council/IRCCS, Istituto Ortopedico Rizzoli, 40136 Bologna, Italy

[5]Department of Neuroscience, International School for Advanced Studies (SISSA), 34136 Trieste, Italy

[6]Department of Life Sciences, University of Trieste, 34128 Trieste, Italy

[7]Department of Cellular, Computational and Integrative Biology (CIBIO), University of Trento, Povo, 38123 TN, Italy

[8]These authors contributed equally

[9]Lead contact

*Correspondence: marco.canossa@unitn.it (M.C.), cher@sissa.it (E.C.)

https://doi.org/10.1016/j.isci.2022.105728

cognitive processes.[20] It is worth mentioning that in these animals, protein trafficking from the endo-plasmatic reticulum to the membrane is severely impaired and only a small fraction of the protein (<10%) reaches the membrane. This small fraction loses its capacity to dimerize and to bind β-neurexin, thus altering information and cognitive processes.[5] Similarly, to NLG3^{R451C} KI mice, NLG3 knock-out (NLG3 KO) mice,[13] recapitulate several behavioral deficits of ASDs, particularly those related to social cognition.[21–23] Therefore, these mice are considered very informative animal models for ASD pathogenesis.[24]

Here, we progressed from the general idea that activity-dependent alterations in synaptic plasticity represent a convergent mechanism underlying several neuro-developmental disorders including ASDs.[13] We tested the hypothesis that a disruption of GABAergic signaling, early in postnatal development, may affect spike time dependent plasticity (STDP), a particular Hebbian form of learning, crucial for information coding. STDP consists in bidirectional modifications of synaptic strength, which rely on the temporal order of pre and postsynaptic spiking.[25] Thus, positively correlated pre and postsynaptic spiking (pre before post) within a critical window leads to LTP whereas a negative correlation (post before pre) to LTD.[26–29]

We found that neonatal NLG3^{R451C} KI mice, which exhibit a premature hyperpolarizing action of GABA at immature MF-CA3 synapses, failed to develop STD-LTP. This effect, which persisted in adulthood, was associated with significant reduction of TrkB phosphorylation at potentiated synapses. A similar cohort of events was found in NLG3 KO mice, suggesting a loss of function. Thus, perturbation of GABAergic phenotype at early developmental stages provides the ground for persistent alterations of synaptic plasticity in the hippocampus of animal models of Autism.

RESULTS

Early hyperpolarizing action of GABA at MF-CA3 synapses of neonatal NLG3^{R451C} KI mice

Early in postnatal development, GABA, acting on $GABA_A$ receptors, depolarizes and excites targeted cells by an outwardly directed flux of Cl^-.[30] This phenomenon is due to the high levels of intracellular Cl^- that result from the differential temporal expression of the cation-chloride co-transporters NKCC1 and KCC2, which are involved in Cl^- uptake and extrusion, respectively.[31] Intracellular calcium rise, following activation of NMDA receptors and voltage-dependent calcium channels, associated with the depolarizing and excitatory action of GABA, contributes to synaptic wiring and refinement of local neuronal circuits.[32–34] A persistent depolarizing action of GABA into adulthood has been found to be associated with several neurodevelopmental disorders,[35–37] including ASDs.[38]

Therefore, we first tested the direction of GABA action at immature mossy fibers (MF)-CA3 synapses in NLG3^{R451C} KI mice, known to exhibit, at early developmental stages, a GABAergic phenotype.[39,40] $GABA_A$-mediated postsynaptic currents (GPSCs) were recorded at MF-CA3 synapses in hippocampal slices obtained from NLG3^{R451C} KI mice and littermate controls, using gramicidin-perforated patch, to prevent changes in intracellular chloride concentration. Unexpectedly at P2-P7, stimulation of granule cells in the DG of NLG3^{R451C} KI mice, evoked in CA3 principal cells synaptic responses whose reversal (E_{GPSCs}) was shifted toward more hyperpolarized values respect to controls (Figure 1A). The equilibrium potential of MF-GPSCs was -50.9 ± 3.0 mV and -39.7 ± 3.2 mV in NLG3^{R451C} KI and control mice, respectively, while similar values of resting membrane potential (RMP), estimated at the end of the experiments by breaking the membrane, were observed in the two phenotypes (-46.6 ± 1.7 mV and -47.2 ± 1.7 mV in NLG3^{R451C} KI and control mice, respectively). The RMP was used to measure the driving force for MF- GPSCs (ΔF_{GABA}), being $\Delta F_{GABA} = E_{GPCs}$-RMP. ΔF_{GABA} values from controls and NLG3^{R451C} KI mice were significantly different (4.38 ± 3.0 and -7.71 ± 3.1, respectively; Figure 1B). Thus, in this animal model of autism, early in postnatal life, GABA released from mossy fibers terminals atypically exerts on targeted neurons a hyperpolarizing type of action.

Loss of STD-LTP at immature GABAergic MF-CA3 synapses of NLG3^{R451C} KI mice

The premature shift of GABA from the depolarizing to the hyperpolarizing direction observed in NLG3^{R451C} KI mice may affect synaptic connectivity and plasticity processes at MF-CA3 connections. Therefore, in the following experiments, we tested whether these synapses could be potentiated following STD-LTP protocol. To this aim, GPSCs elicited by minimal stimulation of granule cells in the dentate gyrus (at 0.05 Hz) were recorded at −70 mV in CA3 pyramidal cells of hippocampal slices obtained from postnatal (P) day P2–P7 NLG3^{R451C} KI mice and control littermates (Figure 2A). After a control period of 10 min, STDP was induced

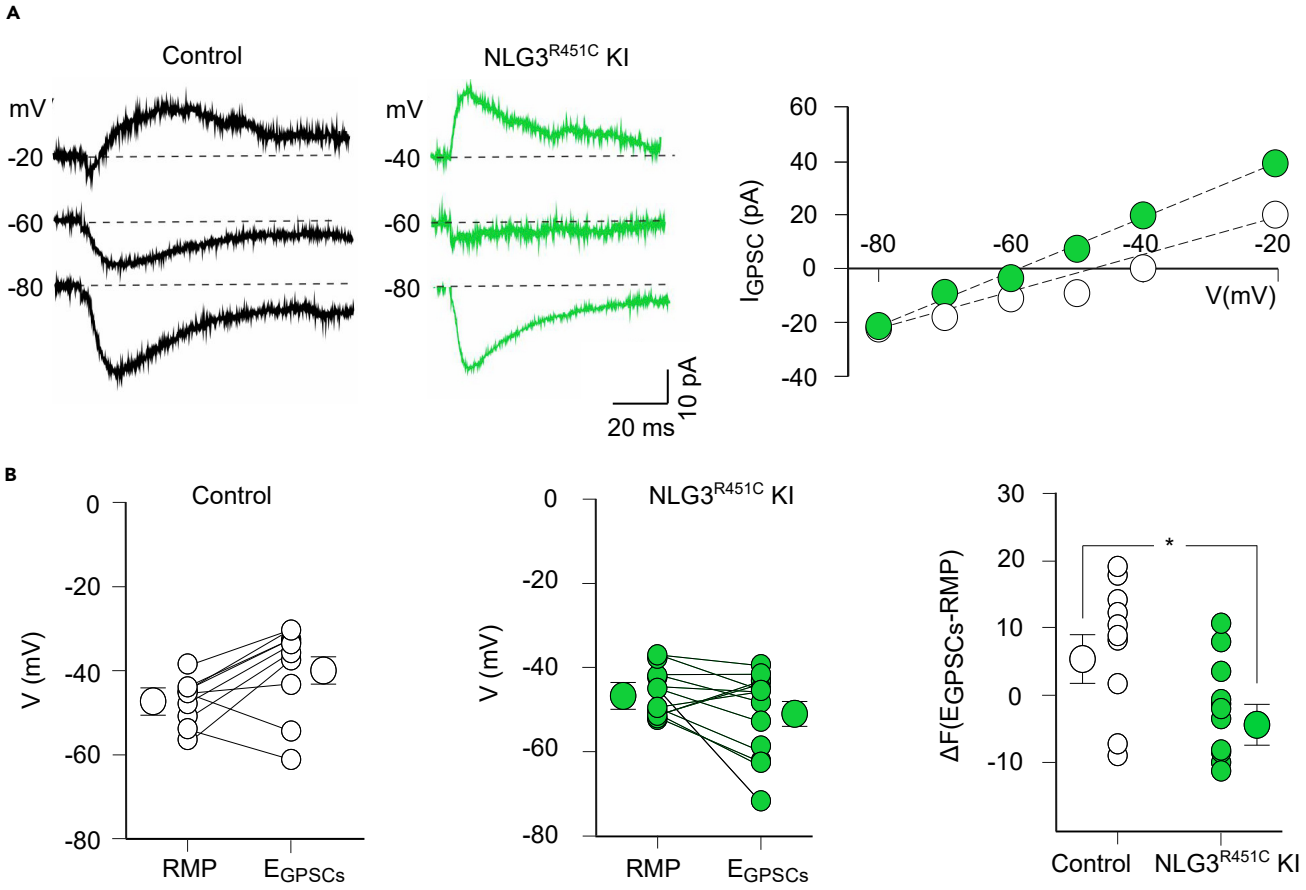

Figure 1. Early hyperpolarizing action of GABA at immature MF-CA3 synapses of NLG3^{R451C} KI mice

(A) Representative traces of MF-GPSCs evoked at three different holding potentials in CA3 principal cells by stimulation of granule cells in the DG (gramicidin-perforated patches) in controls (black) and in NLG3^{R451C} KI mice (green). On the right, the amplitudes of MF-GPSCs are plotted against holding potentials, V(mV).

(B) Individual RMPs and E_{GPSCs} values in CA3 principal cells from littermate controls (black; n = 10 from 3 pups) and NLG3^{R451C} KI mice (green; n = 12 from 6 pups).). Larger symbols on the left and right refer to mean ± SEM values. On the right, the driving force (ΔF) for GABA obtained in individual experiments from controls (black) and NLG3^{R451C} KI mice (green). Larger symbols are mean ± SEM values; *p < 0.05, Wilcoxon test.

in current clamp mode by positively pairing (pre before post) MF-evoked $GABA_A$-mediated postsynaptic potentials (GPSPs) with postsynaptic spikes (10 at 0.1 Hz) with a delay of 15 ms, which corresponds to the peak of MF-GPSP (Figure 2B). Recordings were routinely performed in the presence of DNQX (20 μM) and D-AP5 (50 μM) to block AMPA and NMDA receptors, respectively. In agreement with previous data,[41] the pairing procedure produced in control mice a persistent potentiation (STD-LTP) of MF-GPSCs. Figure 2B shows that 30 min after pairing the peak amplitude of MF-GPSCs was 152.8% of the pre-pairing period (MF-GPSCs increased in amplitude from 59.3 ± 8.0 pA to 90.6 ± 17.9 pA; n = 12; p < 0.01). In agreement to their MF origin, immature GPSCs were sensitive to group III metabotropic glutamate receptor agonist L-AP4 (10 μM).[40] Moreover, they were completely blocked by picrotoxin (PTX, 100 μM) indicating that they were mediated by $GABA_A$ receptors (Figure 2B). This effect was associated with a significant increase in successes rate (from 0.66 ± 0.07 to 0.86 ± 0.05; p < 0.01), suggesting that LTP's expression also involves an enhancement of GABA release. Strikingly, the same procedure failed to induce STD-LTP in NLG3^{R451C} KI mice (Figure 2B). On average, 30 min after pairing the peak amplitude of MF-GPSCs was 98.7% of the pre-pairing period. The peak amplitude of MF-GPSCs varied from 49.3 ± 7.3 pA to 48.6 ± 8.8 pA; n = 12; p = 0.87, before and after pairing, respectively.

To assess whether the loss of STD-LTP observed in NLG3^{R451C} KI mice can be attributed to a loss-of-function, we tested whether a similar impairment of synaptic plasticity occurs in mice lacking the *Nlgn3* gene

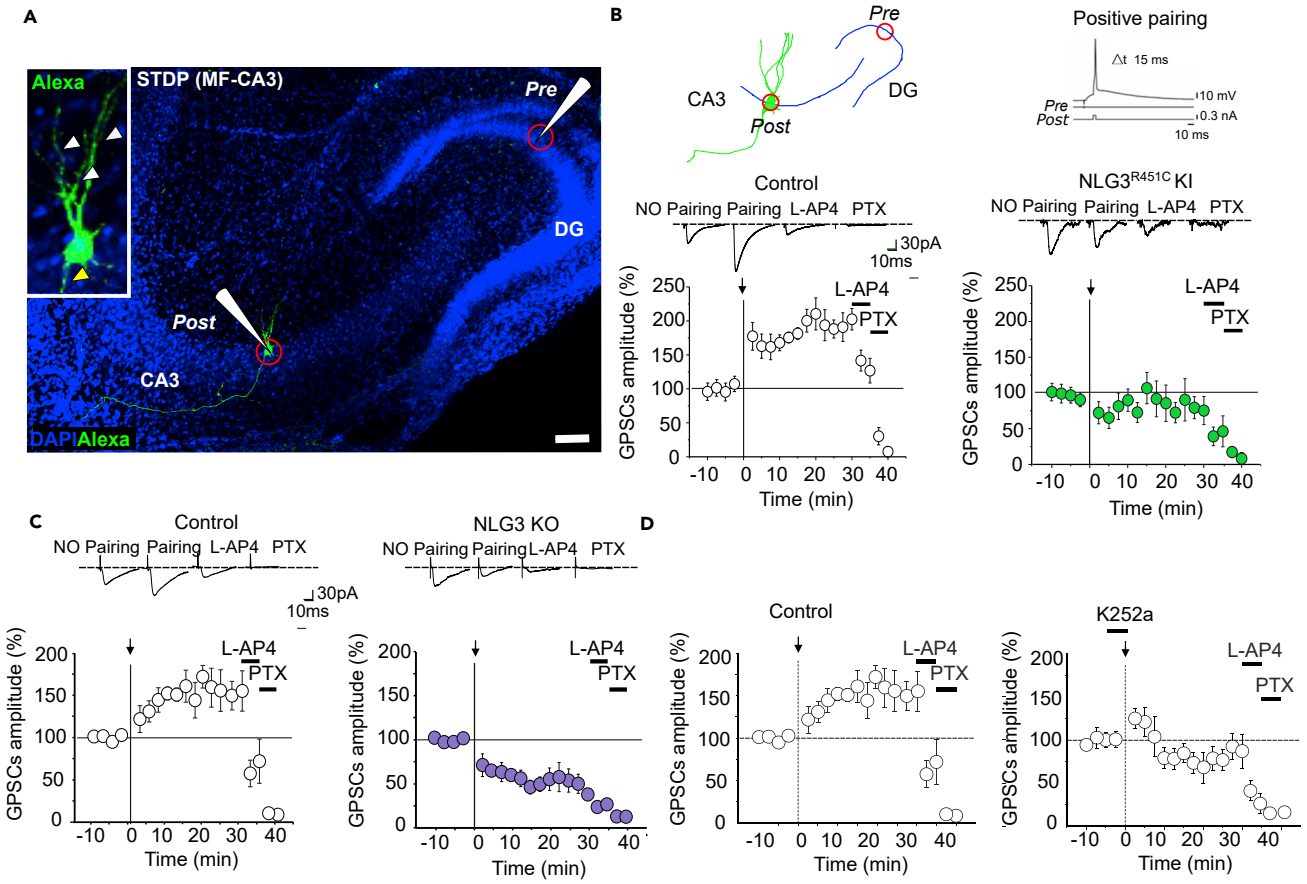

Figure 2. Positive pairing fails to induce STD-LTP at immature MF-GPSCs in NLG3^{R451C} KI and in NLG3 KO mice

(A) Hippocampal slice from a P3 old mouse showing cells (DAPI signal in blue) in the dentate gyrus and the CA3 hippocampal region. Representation of the experimental design with stimulating electrode in the dentate gyrus (pre, red circle) and recording electrode in the pyramidal neuron (post, red circle) are indicated. Inset shows ten times magnification of the neuron subjected to STDP filled with Alexa Fluor 488 (in green). Arrowheads show dendrites oriented toward the stimulation electrode (white) and the axon (yellow) in the opposite direction. Bar is 50 μm.

(B) Schematic representation of the experimental design as in A (upper left). Spike-timing protocol showing the GPSP preceding the postsynaptic spike by 15 ms (Δt) (upper right). Lower graphs show peak amplitude of $GABA_A$-mediated post synaptic currents (GPSCs, expressed as percentage of pre-pairing amplitude), evoked in the presence of DNQX and D-APV, in CA3 principal cells by MF stimulation (pairing: arrows at time 0) as a function of time in hippocampal slices obtained from littermate controls (left) and from NLG3^{R451C} KI mice (right). Insets above the graphs represent averaged MF-GPSCs evoked before (NO pairing), after pairing and in the presence of L-AP4 and PTX.

(C) As in (B), but for MF-GPSCs evoked in littermate controls (left) and in NLG3 KO mice (right). In all cases, MF-GPSCs were sensitive to L-AP4 and were blocked by picrotoxin (PTX) indicating that they were mediated by activation of $GABA_A$ receptors.

(D) Left: peak amplitude of GPSCs evoked in a P3 CA3 principal cells by MF stimulation in hippocampal slices obtained from control animals (littermates of NLG^{R451C} KI mice), expressed as percentage of pre-pairing amplitude in function of time (pairing: arrow at time 0). Right: loss of STD-LTP when the pairing protocol (arrows at time 0) was applied in the presence of the protein tyrosine kinase inhibitor K252a (bar) indicating that expression of STD-LTP depends on the activation of BDNF/TrkB signaling pathway.

(NLG3 KO mice). Figure 2C shows that in these transgenic animals, positive pairing induced a long-lasting depression. On average, 30 min after pairing the peak amplitude of MF-GPSCs was 63.5% of the pre-pairing period (the peak amplitude of MF-GPSCs was 76.3 ± 13.0 pA and 48.5 ± 15.0 pA; n = 7; $p < 0.04$; before and 30 min after pairing, respectively). In contrast, in littermate controls, the same procedure produced a persistent increase in synaptic efficacy (Figure 2C). On average, 30 min after pairing the peak amplitude of MF-GPSCs was 169.0% of the pre-pairing period (the peak amplitude of MF-GPSCs was 52.6 ± 8.0 pA and 88.9 ± 12.7 pA before and after pairing, respectively; n = 6; $p < 0.005$). Finally, in accord with their MF and GABAergic origin, GPSCs, were sensitive to L-AP4 and blocked by picrotoxin (Figure 2C). Overall, these data indicate that functional *Nlgn3* gene is required to generate STD-LTP.

Impairment of TrkB phosphorylation accounts for the loss of STD-LTP in NLG3^{R451C} KI and NLG3 KO mice

In a previous study from rats, we have demonstrated that, at immature GABAergic MF-CA3 synapses, STD-LTP depends on brain-derived neurotrophic factor (BDNF) signaling.[41] To get more insights into the mechanisms underlying the loss of STD-LTP in NLG3^{R451C} KI and NLG3 KO mice, in the next series of experiments we investigated whether the observed changes in synaptic plasticity require BDNF. Initially, the pairing protocol was applied in slices from control mice in presence of the tyrosine kinase inhibitor K252a (Figure 2D) at the concentration of 150 nM[42] to prevent phosphorylation of the BDNF receptor TrkB.[43] K252a was applied in the bath 5 min before pairing and it was washed out immediately after. Figure 2D shows that K252a prevents synaptic potentiation, indicating that STD-LTP closely depends on TrkB signaling pathway.

We then hypothesized that BDNF, released during spike-induced membrane depolarization would activate LTP-related signaling pathways via TrkB initial phosphorylation. We focused on TrkB receptors present at postsynaptic sites of principal cells exposed to the pairing procedure. The STDP protocol was applied to CA3 principal cells intracellularly labeled with Alexa Fluor 488 dye for post-hoc identification of the recorded neurons. To evaluate the effects of the pairing procedure on the activation of TrkB in neurons subjected to STDP, hippocampal slices from control and NLG3 mutant mice were then immunoassayed for TrkB phosphorylation (pTrkB) by using α-phospho-TrkB (Tyr816) antibody (αpTrkB). Spatial co-localization of pTrkB at postsynaptic sites was obtained by co-localizing pTrkB signal with that of the postsynaptic density marker, PSD95. This postsynaptic protein is first encountered in early developing synapses and it is attached under the surface of the postsynaptic membrane across from a vesicle-containing presynaptic axon.[44] Moreover, PSD95 is usually associated with glutamatergic AMPA receptor expression, which coexists with $GABA_A$ receptors on dendritic spines of immature CA3 principal cells.[45] pTrkB/PSD95 co-localization was initially analyzed in a series of confocal stacks (z-stacks) in different regions of interests (ROIs) of the STDP neurons including the dendritic subcellular region (ROI 1) oriented toward the site of stimulation (Figure S1A). For quantification analysis we used Mander's overlap that accounts the abundance of fluorophores that overlap with each other.[46] Using this analytical tool, we found that the proportion of pTrkB/PSD95 co-localization was increased in the dendritic subcellular region of slices from control mice exposed to the pairing protocol as compared to those not subjected to pairing, confirming the involvement of TrkB signaling in STD-LTP (Figure S1B). The specificity of pTrkB signal in principle neurons exposed to the pairing protocol was controlled by measuring pTrkB/PSD95 co-localization in an enlarged area comprising the stimulated and non-stimulated CA3 pyramidal cells (ROI 2). Here, levels of pTrkB/PSD95 co-localization resulted not significantly changed from control unstimulated neurons suggesting that phosphorylation of the receptors can only be observed at the connecting sites in response to STDP (Figure S1B).

In developing hippocampal neurons most synapses are known to form on dendritic shafts, which then mature into morphologically well-defined dendritic spines during the first 2–3 postnatal weeks.[44] Accordingly, at P0-P7 spines morphology is hardly visible at the light microscopic level including confocal microscopy. To evaluate the effects of the pairing procedure on the phosphorylation of TrkB receptors present on single postsynaptic sites of CA3 neurons subjected to STDP, we first co-localized PSD95 and Alexa Fluor 488 signals and then selected PSD95/Alexa 488 co-localization signals only expressing pTrkB in each analyzed confocal stack (Figures S2A and S2B). Only complete overlapping of pTrkB immunoreactivity with PSD95/Alexa 488 co-localization signal was considered an activated spine (Figure S2C). As compared to the pre-pairing conditions, CA3 principal cells from control mice exposed to STD-LTP, exhibited a significant increase of PSD95/Alexa 488 co-localization signals expressing pTrkB, suggesting that indeed STD-LTP induces TrkB activation in dendritic spines of CA3 principal cells (Figures 3A, 3C, and 3F). In strike contrast, in neurons subjected to STDP from NLG3^{R451C} KI (Figures 3D and 3F) and NLG3 KO mice (Figures 3E and 3F), the percentage of PSD95/Alexa 488 co-localization signals expressing pTrkB after pairing was not different from that of unstimulated controls (Figures 3B and 3F). Thus, the observed deficit in synaptic plasticity observed in transgenic mice is associated with a loss of active spines in STDP neurons. Active spines were further resolved in super-resolution (Figure 4A) by using three-dimensional structured illumination microscopy (3D-SIM) for their qualitative morphological reconstruction. In control neurons subjected to STD-LTP, Alexa 488/PSD95/pTrkB tri-co-localization signals (Figure 4B) appeared largely diffused along processes and higher magnification allowed visualization of some clusters of pTrkB positive spines (Figures 4C and S3).

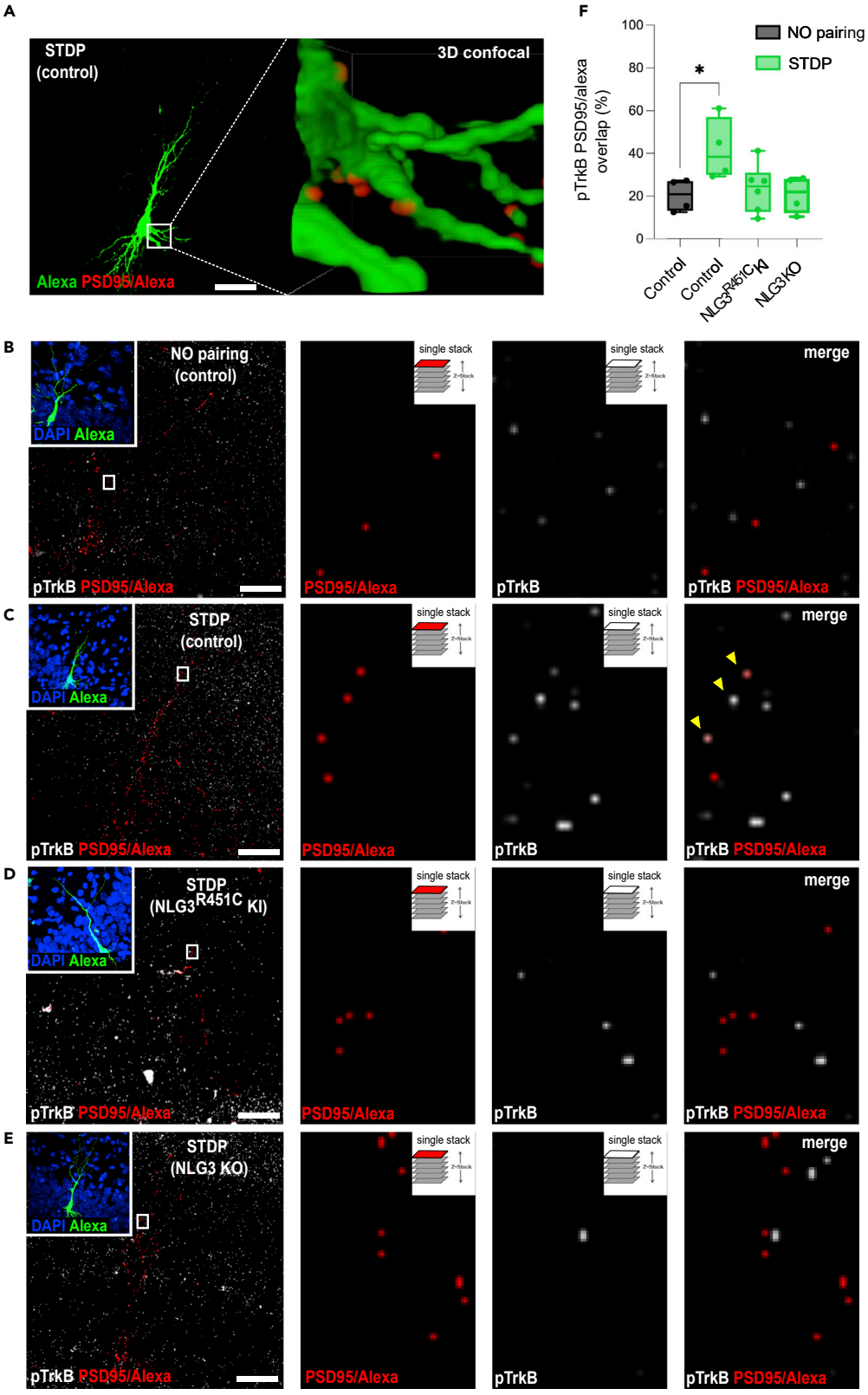
A
STDP
(control)
3D confocal
Alexa PSD95/Alexa
F
NO pairing
STDP
pTrkB PSD95/alexa
overlap (%)
100
80
60
40
20
0
*
Control
Control
NLG3R451C KI
NLG3KO
B
NO pairing
(control)
DAPI Alexa
pTrkB PSD95/Alexa
single stack
PSD95/Alexa
pTrkB
merge
C
STDP
(control)
D
STDP
(NLG3R451C KI)
E
STDP
(NLG3 KO)

Figure 3. TrkB phosphorylation on dendritic spines of CA3 pyramidal neurons subjected to STDP

(A) 3D-reconstruction of Alexa Fluor 488 (green) and PSD95/Alexa co-localization signal (red) of the same neuron in (C). Ten-times magnification of proximal dendrites (green) showing PSD95/Alexa co-localization signals (red). Scale bar: 20 μm.

(B) Panel on the left shows 2D-reconstruction (z-stacks) of pTrkB (white) and PSD95/Alexa co-localization signals (red) in a CA3 principal neuron, filled with Alexa Fluor 488 not subjected to the pairing protocol in a slice from a control mouse (wild type littermate of NLG3^{R451C} KI mice). The inset shows Alexa Fluor 488 signal (green) and DAPI (blue) of the same neuron. Panels on the right show ten times magnification of a single stack from the region of interest (white rectangle) showing dendritic spines visualized by PSD95/Alexa co-localization signal (red), active spines expressing pTrkB signal (white), and merged images. Scale bar: 10 μm.

(C) As in (B) but for a CA3 principal cell subjected to STDP in a slice from a control mouse (wild type littermate of NLG3^{R451C} KI mice). Note in the right panel merging of two channels allowing identification of dendritic spines expressing pTrkB (yellow arrowheads).

(D) As in (C) but for CA3 pyramidal neurons subjected to STDP protocol in hippocampal slices from NLG3^{R451C} KI mice.

(E) As in (C) but for CA3 pyramidal neurons subjected to STDP protocol in slices from NLG3 KO mice.

(F) The histogram depicts quantification of spines (identified by Alexa 488/GFP co-localization) expressing pTrkB in control littermates not subjected (n = 4, no STDP) or subjected (n = 4, STDP) to the pairing protocol, in NLG3^{R451C} KI (n = 6) and NLG3 KO (n = 4) mice subjected to the pairing protocol (STDP). Note the significant increase in spines phosphorylation only in control mice subjected to pairing inducing LTP. Data are mean ± SEM *$p < 0.05$ (unpaired *t-test*). See also Figures S1 and S2.

Exogenously applied BDNF enhances synaptic efficacy in both NLG3^{R451C} KI and NLG3 KO mice

We hypothesized that the impaired pTrkB in spines and the correlated lack of STD-LTP in NLG3^{R451C} KI and NLG3 KO mice is related to a reduced BDNF availability to STDP neurons during spiking. Hence, BDNF likely released from the postsynaptic neuron during spike-induced membrane depolarization,[47–50] would initiate TrkB phosphorylation that is required for STD-LTP. According to this mechanism, it should be still possible to enhance synaptic efficacy at MF-CA3 synapses of control littermates by exogenously replace BDNF in the absence of pairing stimulation. Figure 5 shows that application of BDNF (40 ng/mL) in the bath for 5 min, was sufficient to significantly increase the amplitude of MF-GPSCs, an effect that persisted for at least 30-40 min after wash. The peak amplitude of MF-GPSCs was 76.1 ± 21.7 pA and 149.9 ± 42.1 pA, before and after BDNF; $p < 0.05$. These results prompted to investigate whether a reduced amount of BDNF during spike-induced membrane depolarization may account for the observed alterations in synaptic plasticity in both NLG3^{R451C} KI and NLG3 KO mice. Accordingly, the application of BDNF (40 ng/mL) in the bath for 5 min, was sufficient to significantly induce a long-lasting increase of MF-GPSCs amplitude in both NLG3^{R451C} KI (Figure 5A) and NLG3 KO mice (Figure 5B). The peak amplitude of MF-GPSCs varied from 50.4 ± 21.2 pA to 100.4 ± 31.02 pA and from 60.12 ± 15.37 pA to 139.4 ± 34.5 pA in NLG3^{R451C} KI and NLG3 KO mice, before and after BDNF, respectively, $p < 0.02$ for both. Thus, reduced BDNF availability is responsible for the STD-LTP deficit in NLG3^{R451C} KI and NLG3 KO mice, a phenotype that could be reversed by exogenous replacement of the neurotrophin.

Positive pairing fails to trigger LTP in adult glutamatergic MF-CA3 synapses of NLG3^{R451C} KI and NLG3 KO mice

Whether the premature shift of GABA from the depolarizing to the hyperpolarizing direction leads to changes in synaptic plasticity that persisted in adulthood was next investigated. In the following experiments, we examined whether STD-LTP failure persisted in adult NLG3^{R451C} KI and NLG3 KO mice, when MF have acquired their glutamatergic phenotype. In adults, the pairing protocol consisted in 60 back propagating action potentials (at 0.1 Hz frequency), delivered 10 ms after presynaptic stimulation of MF in the dentate gyrus.[51] In control animals, the pairing protocol produced synaptic potentiation that persisted for at least 30 min after pairing (Figure 6A). On average, the peak amplitude of MF-EPSCs was 170.9% of the pre-pairing period (the peak amplitude of MF-EPSC was 87.3 ± 21.9 pA and 137.2 ± 34.5 pA before and 30 min after pairing, respectively, n = 5; $p < 0.05$). However, the same pairing protocol failed to induce STD-LTP in adult NLG3^{R451C} KI mice (Figure 6B). On average, 30 min after pairing, the peak amplitude of MF-EPSC was 88% of the pre-pairing period (the peak amplitude of MF-EPSCs was 66.8 ± 12.0 pA and 58.8 ± 7.5 pA before and after pairing, respectively, n = 6; $p = 0.75$). Similar results were obtained from NLG3 KO mice in which, 30 min after pairing, the peak amplitude of MF-EPSC was 71.3% of the pre-pairing period (the peak amplitude of MF-EPSCs was 111.5 ± 14.9 pA and 79.5 ± 21.4 pA before and 30 min after pairing, respectively, n = 5; $p = 0.19$; Figure 6D). In littermate controls the peak amplitude

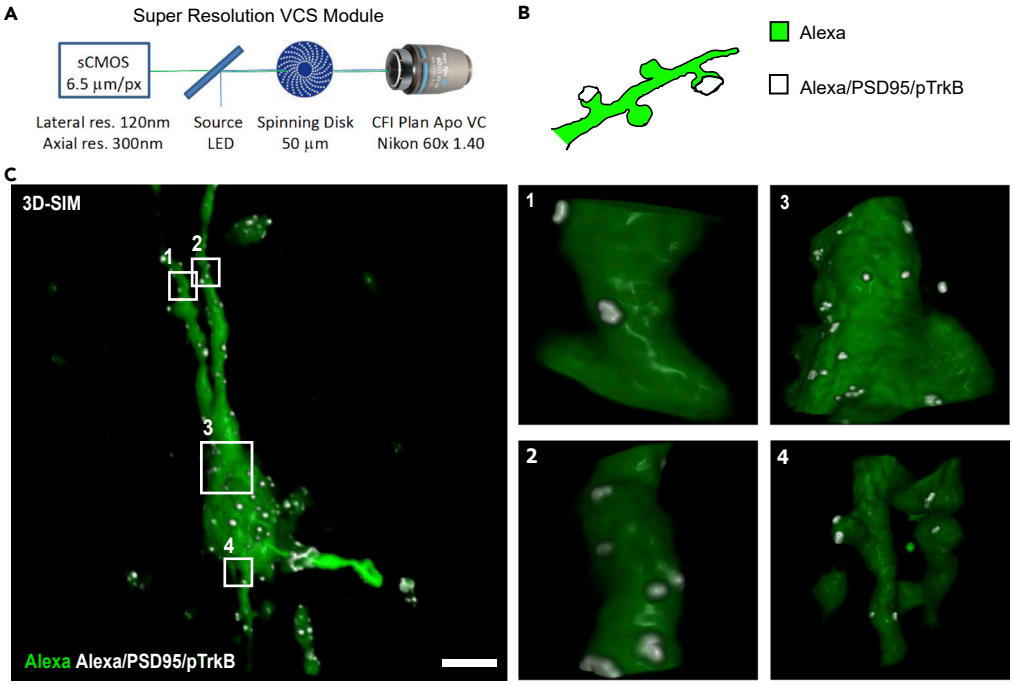

Figure 4. 3D reconstruction of active spines by structured illumination microscopy (SIM)

See also Figure S2.

(A) Schematic representation of the super resolution VCS module.

(B) Schematic representation of 3D-SIM analysis. Tri-co-localization is obtained by combining PSD95/Alexa and pTrkB/PSD95 co-localizations.

(C) 3D reconstruction of Alexa Fluor 488 (green). Ten-times magnification of active spines (1–4) are visualized by PSD95/Alexa /pTrkB tri-co-localization signal (white). Scale bar: 10 µm.

See also Figure S3.

of MF-EPSC was 110.5 ± 7.2 pA and 173.5 ± 17.1 pA before and 30 min after pairing, respectively, (n = 5; p = 0.01; Figure 6C). Thus, perturbation of GABAergic phenotype at early developmental stages provides the ground for persistent impairment of synaptic plasticity at MF-CA3 synapses in adult NLG3^{R451C} KI and NLG3 KO mice, animal models of Autism.

DISCUSSION

The present study from the hippocampus of NLG3^{R451C} KI mouse, an animal model of autism, clearly shows that, early in postnatal development, the premature shift of GABA from the depolarizing to the hyperpolarizing direction affects synaptic plasticity processes, thus preventing the establishment of proper synaptic connections in targeted neurons. A previous study aimed at making GABA hyperpolarizing from birth, by eliminating its excitatory action, by premature expression via *in utero* electroporation of the Cl^- exporter KCC2, led to a severe impairment of morphological maturation of cortical neurons,[52] indicating that the early depolarizing action of GABA is essential for the structural and functional development of neuronal networks. This condition contributes to maintain, within neuronal circuits, a proper excitatory/inhibitory (E/I) balance, essential for nearly all brain functions, including representation of sensory information and cognitive processes.[37] Among different transcriptional regulators of cation-chloride co-transporters, the BDNF-TrkB signaling pathway plays a crucial role.[53] This neurotrophin is instrumental in promoting neuronal growth, differentiation, survival[54] and structural plasticity.[55] BDNF and its receptor TrkB are highly expressed in dentate gyrus granule cells, which regulate the flow of information from the cortex to the hippocampus proper, thus contributing to tune synaptic connectivity involved in learning/memory processes.[56]

In keeping with the key role of BDNF in brain development, we have recently demonstrated that deletion of TrkB from immature dentate granule cells in *Ntrk2/Trkb* mice, during the first postnatal week, when these

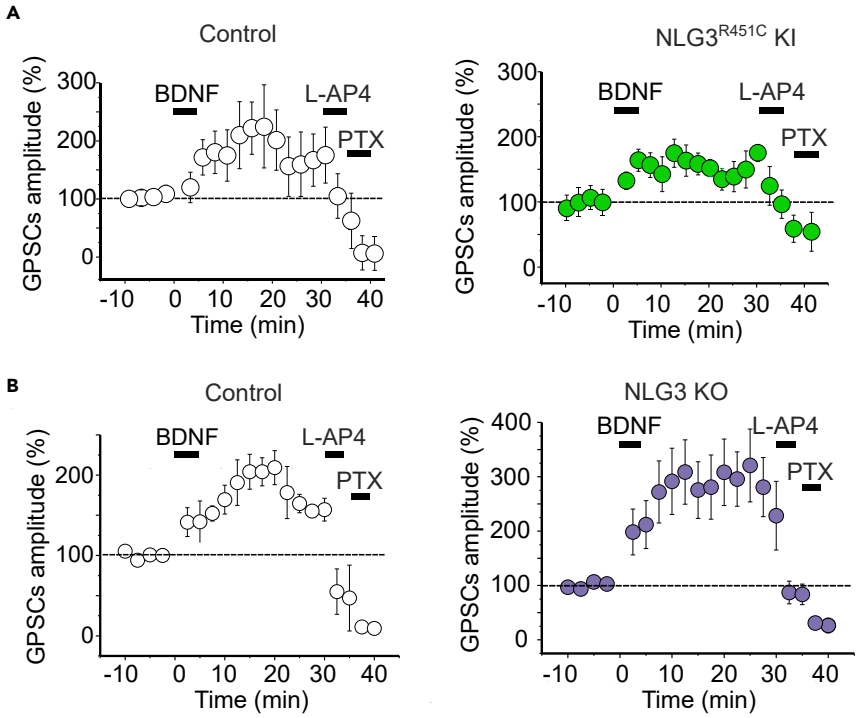

Figure 5. Bath application of BDNF induces synaptic potentiation at immature GABAergic MF-CA3 synapses in both NLG3^{R451C} KI and NLG3 KO mice

(A) Summary plots of mean peak amplitude of MF-GPSCs (expressed as percentage of pre-BDNF treatment), before, during and after bath application of BDNF (bars) in controls (left panels) and NLG3^{R451C} KI (right panel). In agreement with their MF origin, in all animal groups, GABAergic responses were sensitive to group III metabotropic glutamate agonist L-AP4 and were completely blocked by PTX.

(B) as in (A) but for NLG3 KO mice.

cells integrate the hippocampal circuitry, leads to a premature shift of GABA from the depolarizing to the hyperpolarizing direction and structural alterations of downstream neuronal circuits, ultimately affecting hippocampal synaptic plasticity and cognitive processes.[57]

Activity dependent alterations in synaptic plasticity processes represent a convergent mechanism underlying several neuro-developmental disorders including ASDs.[13] Here, NLG3^{R451C} KI mice failed to express STD-LTP at immature hippocampal MF-CA3 synapses, known to exhibit, at early developmental stages, a GABAergic phenotype.[40,58,59] As in the present study, previous data from rat immature hippocampus have clearly demonstrated that STD-LTP requires BDNF, probably released from the recorded neurons during spiking-induced membrane depolarization.[41] Once released, BDNF diffuses away to activate high affinity TrkB receptors localized on both post and presynaptic membranes, and downstream signaling pathways leading to an increased amplitude of synaptic currents and probability of transmitter release, respectively.[33] At the postsynaptic site this effect is regulated by cAMP-dependent PKA,[41] which would enhance the sensitivity to BDNF[60] by increasing TrkB phosphorylation[61] and by recruiting TrkB receptors at dendritic spines.[62] Therefore, it is not surprising that disrupting the BDNF/TrkB signaling pathway during a critical developmental period leads to neurodevelopmental disorders. The failure to induce STD-LTP after positive pairing in the CA3 hippocampal region of both NLG3^{R451C} KI and NLG3 KO mice is probably related to a reduced amount of endogenous BDNF released from CA3 principal cells during spiking, and therefore to the inability of this neurotrophin to activate postsynaptic TrkB receptors and downstream signaling cascades. Although in this study we focused on postsynaptic TrkB receptors, localized on the dendritic spines of Alexa-stained CA3 pyramidal cells, subjected to STDP, we cannot exclude the possibility that the loss of synaptic potentiation is partially due to a concomitant decrease of transmitter release consequent to a reduced activation of presynaptic TrkB receptors by BDNF.[63] The hypothesis that a reduced availability of BDNF at dendritic spines of the activated neuron is responsible for the lack of STD-LTP in NLG3^{R451C}

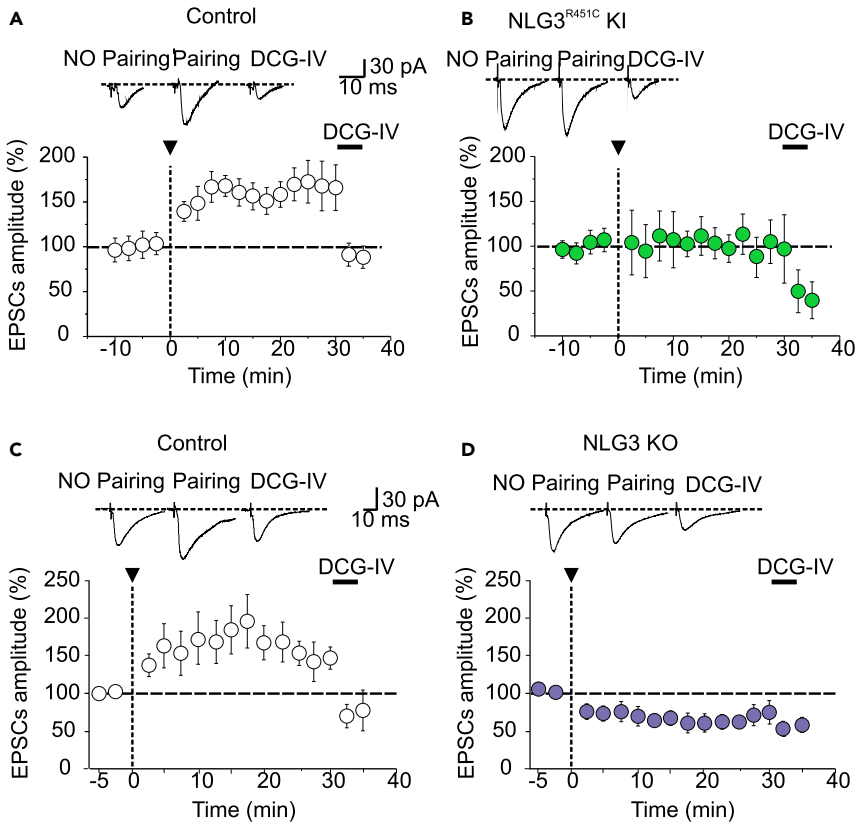

Figure 6. Positive pairing fails to trigger STD-LTP at glutamatergic MF-CA3 synapses in adult NLG3^{R451C} knock-in and NLG3 knock-out mice

(A and B) Summary plots of the mean peak amplitude of MF-EPSCs expressed as percentage of pre-pairing amplitude versus time in controls and in NLG3^{R451C} KI mice (B). Insets above the graphs represent averaged MF-EPSCs evoked NLG3^{R451C} KI mice in controls (No pairing), after pairing and in the presence of group II metabotropic glutamate receptor agonist DCG-IV.

(C and D) as in A-B but for NLG3 KO (D) and control littermates (C). Note that error bars are sometimes within the symbols. Insets above the graphs represent averaged MF-EPSCs evoked in NLG3 KO mice in controls (NO pairing), after pairing and in the presence of group II metabotropic glutamate receptor agonist DCG-IV.

KI and NLG3 KO mice is supported by the experiments in which this phenotype could be reversed by exogenous replacement of this neurotrophin. However, in the present study a direct causal link between changes in BDNF/TrkB signaling and direction of GABA action is lacking, and we cannot exclude the possibility that we are dealing with two parallel processes, caused by the *Nlgn3* gene mutation/loss.

In the immature hippocampus, STD-LTP of GABAergic MF-CA3 synapses is independent on NMDA receptors activation since all experiments were performed in the presence of D-AP5. In contrast with the present experiments from immature GABAergic mossy fibers-CA3 synapses, a previous study from adult NLG3^{R451C} KI, but not NLG3 KO mice,[12] has demonstrated that *stratum radiatum* CA1 synapses, which express a relatively higher number of NR2B-type of NMDA receptors, undergo LTP (in response to three stimulus trains of 100 Hz for 1 s) at least 2-fold larger than controls. In this case, the gain of function responsible for enhancing synaptic plasticity at CA3-CA1 connections might be responsible for the enhanced spatial learning capability in Morris water maze, as it has been shown that the lack of LTP in CA1 is associated with learning deficits in this behavioral task.[10,64] These results suggest that in ASDs, activity-dependent synaptic plasticity processes vary in different brain regions in a developmental dependent cell- and circuit-specific fashion.

In keeping with this, several studies have demonstrated that the NLG3^{R451C} mutation, can cause both gain- and loss-of-function effects, depending on general context and specific alterations in synaptic function that

result in region-specific changes of neural circuits associated with alterations of ASD-relevant mouse behaviors. Unlike Etherton et al. (2011),[12] in our case, the impairment of synaptic potentiation at immature MF-CA3 synapses was present not only on NLG3^{R451C} KI but also on NLG3 KO mice, indicating that this effect was due to a loss of function.

The DG-CA3 pathway is known to play a key role in pattern separation, a cognitive function that allows to prevent overlapping between patterns of neuronal activity representing similar experiences.[65] In addition, evidence has been provided that the DG-CA3-CA2 pathway is crucial for social stimuli discrimination,[66] altered in both NLG3^{R451C} KI and NLG3 KO mice.[12,21–23] Therefore, disrupting the flow of information from the DG to the hippocampus proper, as observed in the present case, may contribute to impair pattern separation and social behavior, which constitutes a core symptom of ASDs.

As already mentioned, the early hyperpolarizing action of GABA at immature mossy fibers-CA3 synapses would prevent the establishment of proper synaptic connectivity in targeted neurons.[52,57] In particular, as highlighted in Badurek et al. (2020),[57] structural changes may affect downstream signaling pathways and cognitive abilities in adulthood. In addition, we cannot exclude the possibility that changes in synaptic strength influence other brain areas connected to the hippocampus such as the entorhinal cortex and the amygdala. As a matter of speculation, we believe that these alterations may constitute putative general mechanisms in neurodevelopmental disorders including those forms of ASDs caused by synaptic dysfunction.

The persistence of STD-LTP impairment in adult NLG3^{R451C} KI and NLG3 KO mice, when MF-CA3 synapses have acquired a glutamatergic phenotype, allows us to hypothesize the occurrence of structural changes, probably related to alterations of BDNF/TrkB signaling pathways. In support of this assumption, immunostaining, and high-resolution microscopy of CA3 principal neurons from control animals exposed to the pairing protocol (identified by intracellular labeling with Alexa Fluor 488 dye), have clearly demonstrated an increased number of spines expressing TrkB phosphorylation on CA3 pyramidal cell dendrites of littermate controls but not NLG3^{R451C} KI and NLG3 KO mice.

Interestingly, in line with the present results, newborn children, later diagnosed with ASDs, have been found to express low blood levels of BDNF.[67] Since BDNF can cross the blood brain barrier,[68] its concentration in the blood probably reflects the concentration in the brain. Neurodevelopmental disorders which initiate during pregnancy[69] are possibly associated with low BDNF levels already *in utero*. Therefore, BDNF levels can be used as biomarkers for the early identification of neonates at high risk for ASDs, thus paving the way to the early diagnosis and treatment of these disorders.

In conclusions, our data shows for the first time that the early shift of GABA from the depolarizing to the hyperpolarizing direction, likely related to deficits of BDNF/TrkB signaling leads, as the persistent depolarizing action of this neurotransmitter in adulthood[34,37] to Neurodevelopmental Disorders, further highlighting the key role of a proper GABAergic signaling in brain development.

Limitations of the study

It is worth mentioning that, while it is well known that BDNF/TrkB signaling controls the direction of $GABA_A$-mediated neurotransmission acting on the cation-chloride exporter KCC2,[70–72] the impact of this neurotrophin on the cation-chloride importer NKCC1 has been only recently unveiled.[57,73] However, in the present study the mechanism by which, early in postnatal development, the impairment of BDNF/TrkB signaling alters the expression of NKCC1 in the hippocampus leading to a premature shift of GABA from the depolarizing to the hyperpolarizing direction has not been addressed and will be the object of future investigations.

STAR★METHODS

Detailed methods are provided in the online version of this paper and include the following:

- KEY RESOURCES TABLE
- RESOURCE AVAILABILITY
  - Lead contact
  - Materials availability

SUPPLEMENTAL INFORMATION

Supplemental information can be found online at https://doi.org/10.1016/j.isci.2022.105728.

ACKNOWLEDGMENTS

We are grateful to members of our lab for providing valuable discussion, technical advice, and feedback on the manuscript.This research was funded by: Progetti di Ricerca di Rilevanza Nazionale (PRIN) grant 2017 HPTFFCPRIN to MC; European Research Council (ERC) under the European Union's Horizon 2020 research and innovation program grant 788793-BACKUP to BV and MC; EU Horizon 2020, Human Brain Project (HBP, SGA2) grant 785907to EC; Telethon grant, GGP 16083 to EC; Fondo Ordinario Enti (FOE)-CNR/EBRI, DM 865/2019 to EC, CM and MG.

AUTHOR CONTRIBUTIONS

Conceptualization: EC, MC, MG, CM, BV, Methodology: DP; MG; MS; BV; AB; GW, Validation: FM, SS, BV, PZ, Formal analysis: MG, CM, DP, MS, BV, Investigation: EC, MC, MG, CM, BV, Resources: EC, MC, MG, CM, BV, Data curation: EC, MC, MG, DP, MS, BV, Writing-original draft preparation: EC, MC, BV, Writing-review and editing: EC, MC, BV.

All authors have read and agreed to the published version of the manuscript.

DECLARATION OF INTERESTS

The authors declare no competing interests.

Received: August 8, 2022
Revised: October 25, 2022
Accepted: December 1, 2022
Published: January 20, 2023

REFERENCES

1. Zoghbi, H.Y., and Bear, M.F. (2012). Synaptic dysfunction in neurodevelopmental disorders associated with autism and intellectual disabilities. Cold Spring Harbor Perspect. Biol. *4*, a009886. https://doi.org/10.1101/cshperspect.a009886.

2. Banerjee, S., Riordan, M., and Bhat, M.A. (2014). Genetic aspects of autism spectrum disorders: insights from animal models. Front. Cell. Neurosci. *8*, 58. https://doi.org/10.3389/fncel.2014.00058.

3. Guang, S., Pang, N., Deng, X., Yang, L., He, F., Wu, L., Chen, C., Yin, F., and Peng, J. (2018). Synaptopathology involved in autism spectrum disorder. Front. Cell. Neurosci. *12*, 470. https://doi.org/10.3389/fncel.2018.00470.

4. Quesnel-Vallières, M., Weatheritt, R.J., Cordes, S.P., and Blencowe, B.J. (2019). Autism spectrum disorder: insights into convergent mechanisms from transcriptomics. Nat. Rev. Genet. *20*, 51–63. https://doi.org/10.1038/s41576-018-0066-2.

5. Südhof, T.C. (2008). Neuroligins and neurexins link synaptic function to cognitive disease. Nature *455*, 903–911. https://doi.org/10.1038/nature07456.

6. Bourgeron, T. (2009). A synaptic trek to autism. Curr. Opin. Neurobiol. *19*, 231–234. https://doi.org/10.1016/j.conb.2009.06.003.

7. Jamain, S., Quach, H., Betancur, C., Råstam, M., Colineaux, C., Gillberg, I.C., Soderstrom, H., Giros, B., Leboyer, M., Gillberg, C., et al. (2003). Mutations of the X-linked genes encoding neuroligins NLGN3 and NLGN4 are associated with autism. Nat. Genet. *34*, 27–29. https://doi.org/10.1038/ng1136.

8. Gilman, S.R., Iossifov, I., Levy, D., Ronemus, M., Wigler, M., and Vitkup, D. (2011). Rare de novo variants associated with autism implicate a large functional network of genes involved in formation and function of synapses. Neuron *70*, 898–907. https://doi.org/10.1016/j.neuron.2011.05.021.

9. Sanders, S.J., Ercan-Sencicek, A.G., Hus, V., Luo, R., Murtha, M.T., Moreno-De-Luca, D.,

Chu, S.H., Moreau, M.P., Gupta, A.R., Thomson, S.A., et al. (2011). Multiple recurrent de novo CNVs, including duplications of the 7q11.23 williams syndrome region, are strongly associated with autism. Neuron *70*, 863–885. https://doi.org/10.1016/j.neuron.2011.05.002.

10. Tabuchi, K., Blundell, J., Etherton, M.R., Hammer, R.E., Liu, X., Powell, C.M., and Südhof, T.C. (2007). A neuroligin-3 mutation implicated in autism increases inhibitory synaptic transmission in mice. Science *318*, 71–76. https://doi.org/10.1126/science.1146221.

11. Chadman, K.K., Gong, S., Scattoni, M.L., Boltuck, S.E., Gandhy, S.U., Heintz, N., and Crawley, J.N. (2008). Minimal aberrant behavioral phenotypes of neuroligin-3 R451C knockin mice. Autism Res. *1*, 147–158. https://doi.org/10.1002/aur.22.

12. Etherton, M., Földy, C., Sharma, M., Tabuchi, K., Liu, X., Shamloo, M., Malenka, R.C., and Südhof, T.C. (2011). Autism-linked neuroligin-3 R451C mutation differentially alters hippocampal and cortical synaptic function. Proc. Natl. Acad. Sci. USA *108*, 13764–13769. https://doi.org/10.1073/pnas.1111093108.

13. Baudouin, S.J., Gaudias, J., Gerharz, S., Hatstatt, L., Zhou, K., Punnakkal, P., Tanaka, K.F., Spooren, W., Hen, R., De Zeeuw, C.I., et al. (2012). Shared synaptic pathophysiology in syndromic and nonsyndromic rodent models of autism. Science *338*, 128–132. https://doi.org/10.1126/science.1224159.

14. Pizzarelli, R., and Cherubini, E. (2013). Developmental regulation of GABAergic signalling in the hippocampus of neuroligin 3 R451C knock-in mice: an animal model of Autism. Front. Cell. Neurosci. *7*, 85. https://doi.org/10.3389/fncel.2013.00085.

15. Jaramillo, T.C., Liu, S., Pettersen, A., Birnbaum, S.G., and Powell, C.M. (2014). Autism-related neuroligin-3 mutation alters social behavior and spatial learning: neuroligin-3 point mutant behavior. Autism Res. *7*, 264–272. https://doi.org/10.1002/aur.1362.

16. Polepalli, J.S., Wu, H., Goswami, D., Halpern, C.H., Südhof, T.C., and Malenka, R.C. (2017). Modulation of excitation on parvalbumin interneurons by neuroligin-3 regulates the hippocampal network. Nat. Neurosci. *20*, 219–229. https://doi.org/10.1038/nn.4471.

17. Földy, C., Malenka, R.C., and Südhof, T.C. (2013). Autism-associated neuroligin-3 mutations commonly disrupt tonic endocannabinoid signaling. Neuron *78*, 498–509. https://doi.org/10.1016/j.neuron.2013.02.036.

18. Cellot, G., and Cherubini, E. (2014). Reduced inhibitory gate in the barrel cortex of Neuroligin3 ^{R451C} knock-in mice, an animal model of autism spectrum disorders. Phys. Rep. *2*, e12077. https://doi.org/10.14814/phy2.12077.

19. Fricker, D., and Miles, R. (2000). EPSP amplification and the precision of spike timing in hippocampal neurons. Neuron *28*, 559–569. https://doi.org/10.1016/S0896-6273(00)00133-1.

20. Uhlhaas, P.J., and Singer, W. (2006). Neural synchrony in brain disorders: relevance for cognitive dysfunctions and pathophysiology. Neuron *52*, 155–168. https://doi.org/10.1016/j.neuron.2006.09.020.

21. Radyushkin, K., Hammerschmidt, K., Boretius, S., Varoqueaux, F., El-Kordi, A., Ronnenberg, A., Winter, D., Frahm, J., Fischer, J., Brose, N., and Ehrenreich, H. (2009). Neuroligin-3-deficient mice: model of a monogenic heritable form of autism with an olfactory deficit. Gene Brain Behav. *8*, 416–425. https://doi.org/10.1111/j.1601-183X.2009.00487.x.

22. Bariselli, S., Hörnberg, H., Prévost-Solié, C., Musardo, S., Hatstatt-Burklé, L., Scheiffele, P., and Bellone, C. (2018). Role of VTA dopamine neurons and neuroligin 3 in sociability traits related to nonfamiliar conspecific interaction. Nat. Commun. *9*, 3173. https://doi.org/10.1038/s41467-018-05382-3.

23. Modi, B., Pimpinella, D., Pazienti, A., Zacchi, P., Cherubini, E., and Griguoli, M. (2019). Possible implication of the CA2 hippocampal circuit in social cognition deficits observed in the neuroligin 3 knock-out mouse, a non-syndromic animal model of autism. Front. Psychiatr. *10*, 513. https://doi.org/10.3389/fpsyt.2019.00513.

24. Rothwell, P.E., Fuccillo, M.V., Maxeiner, S., Hayton, S.J., Gokce, O., Lim, B.K., Fowler, S.C., Malenka, R.C., and Südhof, T.C. (2014). Autism-associated neuroligin-3 mutations commonly impair striatal circuits to boost repetitive behaviors. Cell *158*, 198–212. https://doi.org/10.1016/j.cell.2014.04.045.

25. Dan, Y., and Poo, M.-M. (2006). Spike timing-dependent plasticity: from synapse to perception. Physiol. Rev. *86*, 1033–1048. https://doi.org/10.1152/physrev.00030.2005.

26. Markram, H., Lübke, J., Frotscher, M., and Sakmann, B. (1997). Regulation of synaptic efficacy by coincidence of postsynaptic APs and EPSPs. Science *275*, 213–215. https://doi.org/10.1126/science.275.5297.213.

27. Bi, G.Q., and Poo, M.M. (1998). Synaptic modifications in cultured hippocampal neurons: dependence on spike timing, synaptic strength, and postsynaptic cell type. J. Neurosci. *18*, 10464–10472. https://doi.org/10.1523/JNEUROSCI.18-24-10464.1998.

28. Debanne, D., Gähwiler, B.H., and Thompson, S.M. (1998). Long-term synaptic plasticity between pairs of individual CA3 pyramidal cells in rat hippocampal slice cultures. J. Physiol. *507*, 237–247. https://doi.org/10.1111/j.1469-7793.1998.237bu.x.

29. Feldman, D.E. (2012). The spike-timing dependence of plasticity. Neuron *75*, 556–571. https://doi.org/10.1016/j.neuron.2012.08.001.

30. Ben-Ari, Y., Cherubini, E., Corradetti, R., and Gaiarsa, J.L. (1989). Giant synaptic potentials in immature rat CA3 hippocampal neurones. J. Physiol. *416*, 303–325. https://doi.org/10.1113/jphysiol.1989.sp017762.

31. Rivera, C., Voipio, J., Payne, J.A., Ruusuvuori, E., Lahtinen, H., Lamsa, K., Pirvola, U., Saarma, M., and Kaila, K. (1999). The K+/Cl− co-transporter KCC2 renders GABA hyperpolarizing during neuronal maturation. Nature *397*, 251–255. https://doi.org/10.1038/16697.

32. Kasyanov, A.M., Safiulina, V.F., Voronin, L.L., and Cherubini, E. (2004). GABA-mediated giant depolarizing potentials as coincidence detectors for enhancing synaptic efficacy in the developing hippocampus. Proc. Natl. Acad. Sci. USA *101*, 3967–3972. https://doi.org/10.1073/pnas.0305974101.

33. Mohajerani, M.H., Sivakumaran, S., Zacchi, P., Aguilera, P., and Cherubini, E. (2007). Correlated network activity enhances synaptic efficacy via BDNF and the ERK pathway at immature CA3–CA1 connections in the hippocampus. Proc. Natl. Acad. Sci. USA *104*, 13176–13181. https://doi.org/10.1073/pnas.0704533104.

34. Ben-Ari, Y., Khalilov, I., Kahle, K.T., and Cherubini, E. (2012). The GABA excitatory/inhibitory shift in brain maturation and neurological disorders. Neuroscientist *18*, 467–486. https://doi.org/10.1177/1073858412438697.

35. Deidda, G., Parrini, M., Naskar, S., Bozarth, I.F., Contestabile, A., and Cancedda, L. (2015). Reversing excitatory GABAAR signaling restores synaptic plasticity and memory in a mouse model of Down syndrome. Nat. Med. *21*, 318–326. https://doi.org/10.1038/nm.3827.

36. Kim, H.R., Rajagopal, L., Meltzer, H.Y., and Martina, M. (2021). Depolarizing GABA $_A$ current in the prefrontal cortex is linked with cognitive impairment in a mouse model relevant for schizophrenia. Sci. Adv. *7*, eaba5032. https://doi.org/10.1126/sciadv.aba5032.

37. Cherubini, E., Di Cristo, G., and Avoli, M. (2021). Dysregulation of GABAergic signaling in neurodevelomental disorders: targeting cation-chloride Co-transporters to Re-establish a proper E/I balance. Front. Cell. Neurosci. *15*, 813441. https://doi.org/10.3389/fncel.2021.813441.

38. Tyzio, R., Nardou, R., Ferrari, D.C., Tsintsadze, T., Shahrokhi, A., Eftekhari, S., Khalilov, I., Tsintsadze, V., Brouchoud, C., Chazal, G., et al. (2014). Oxytocin-mediated GABA inhibition during delivery attenuates autism pathogenesis in rodent offspring. Science *343*, 675–679. https://doi.org/10.1126/science.1247190.

39. Safiulina, V.F., Caiati, M.D., Sivakumaran, S., Bisson, G., Migliore, M., and Cherubini, E. (2010). Control of GABA release at single mossy fiber-CA3 connections in the developing hippocampus. Front. Synaptic Neurosci. *2*, 1. https://doi.org/10.3389/neuro.19.001.2010.

40. Safiulina, V.F., Fattorini, G., Conti, F., and Cherubini, E. (2006). GABAergic signaling at mossy fiber synapses in neonatal rat Hippocampus. J. Neurosci. *26*, 597–608. https://doi.org/10.1523/JNEUROSCI.4493-05.2006.

41. Sivakumaran, S., Mohajerani, M.H., and Cherubini, E. (2009). At immature mossy-fiber-CA3 synapses, correlated presynaptic and postsynaptic activity persistently enhances GABA release and network excitability via BDNF and cAMP-dependent PKA. J. Neurosci. *29*, 2637–2647. https://doi.org/10.1523/JNEUROSCI.5019-08.2009.

42. Knüsel, B., and Hefti, F. (1992). K-252 compounds: modulators of neurotrophin signal transduction. J. Neurochem. *59*, 1987–1996. https://doi.org/10.1111/j.1471-4159.1992.tb10085.x.

43. Bergami, M., Vignoli, B., Motori, E., Pifferi, S., Zuccaro, E., Menini, A., and Canossa, M. (2013). TrkB signaling directs the incorporation of newly generated periglomerular cells in the adult olfactory bulb. J. Neurosci. *33*, 11464–11478. https://doi.org/10.1523/JNEUROSCI.4812-12.2013.

44. Sorra, K.E., and Harris, K.M. (2000). Overview on the structure, composition, function, development, and plasticity of hippocampal dendritic spines. Hippocampus *10*, 501–511. https://doi.org/10.1002/1098-1063(2000)10:5<501::AID-HIPO1>3.0.CO;2-T.

45. Bergersen, L., Ruiz, A., Bjaalie, J.G., Kullmann, D.M., and Gundersen, V. (2003). GABA and GABAA receptors at hippocampal mossy fibre synapses. Eur. J. Neurosci. *18*, 931–941. https://doi.org/10.1046/j.1460-9568.2003.02828.x.

46. Aaron, J.S., Taylor, A.B., and Chew, T.-L. (2018). Image co-localization – co-occurrence versus correlation. J. Cell Sci. *131*, jcs211847. https://doi.org/10.1242/jcs.211847.

47. Goodman, L.J., Valverde, J., Lim, F., Geschwind, M.D., Federoff, H.J., Geller, A.I., and Hefti, F. (1996). Regulated release and polarized localization of brain-derived neurotrophic factor in hippocampal neurons. Mol. Cell. Neurosci. *7*, 222–238. https://doi.org/10.1006/mcne.1996.0017.

48. Lessmann, V., Gottmann, K., and Malcangio, M. (2003). Neurotrophin secretion: current facts and future prospects. Prog. Neurobiol. *69*, 341–374. https://doi.org/10.1016/S0301-0082(03)00019-4.

49. Magby, J.P., Bi, C., Chen, Z.-Y., Lee, F.S., and Plummer, M.R. (2006). Single-cell characterization of retrograde signaling by brain-derived neurotrophic factor. J. Neurosci. *26*, 13531–13536. https://doi.org/10.1523/JNEUROSCI.4576-06.2006.

50. Kuczewski, N., Porcher, C., Ferrand, N., Fiorentino, H., Pellegrino, C., Kolarow, R., Lessmann, V., Medina, I., and Gaiarsa, J.-L. (2008). Backpropagating action potentials trigger dendritic release of BDNF during spontaneous network activity. J. Neurosci. *28*, 7013–7023. https://doi.org/10.1523/JNEUROSCI.1673-08.2008.

51. Astori, S., Pawlak, V., and Köhr, G. (2010). Spike-timing-dependent plasticity in hippocampal CA3 neurons: spike-timing-dependent plasticity in CA3 neurons. J. Physiol. *588*, 4475–4488. https://doi.org/10.1113/jphysiol.2010.198366.

52. Cancedda, L., Fiumelli, H., Chen, K., and Poo, M. -m. (2007). Excitatory GABA action is essential for morphological maturation of cortical neurons in vivo. J. Neurosci. *27*, 5224–5235. https://doi.org/10.1523/JNEUROSCI.5169-06.2007.

53. Rivera, C., Voipio, J., Thomas-Crusells, J., Li, H., Emri, Z., Sipilä, S., Payne, J.A., Minichiello, L., Saarma, M., and Kaila, K. (2004). Mechanism of activity-dependent downregulation of the neuron-specific K-Cl cotransporter KCC2. J. Neurosci. *24*, 4683–4691. https://doi.org/10.1523/JNEUROSCI.5265-03.2004.

54. Binder, D.K., and Scharfman, H.E. (2004). Mini review. Growth Factors *22*, 123–131. https://doi.org/10.1080/08977190410001723308.

55. Park, H., and Poo, M.m. (2013). Neurotrophin regulation of neural circuit development and function. Nat. Rev. Neurosci. *14*, 7–23. https://doi.org/10.1038/nrn3379.

56. Danzer, S.C., Kotloski, R.J., Walter, C., Hughes, M., and McNamara, J.O. (2008). Altered morphology of hippocampal dentate granule cell presynaptic and postsynaptic terminals following conditional deletion of TrkB. Hippocampus *18*, 668–678. https://doi.org/10.1002/hipo.20426.

57. Badurek, S., Griguoli, M., Asif-Malik, A., Zonta, B., Guo, F., Middei, S., Lagostena, L., Jurado-Parras, M.T., Gillingwater, T.H., Gruart, A., et al. (2020). Immature dentate granule cells require ntrk2/trkb for the formation of functional hippocampal circuitry. iScience *23*, 101078. https://doi.org/10.1016/j.isci.2020.101078.

58. Walker, M.C., Ruiz, A., and Kullmann, D.M. (2001). Monosynaptic GABAergic signaling from dentate to CA3 with a pharmacological and physiological profile typical of mossy fiber synapses. Neuron *29*, 703–715. https://doi.org/10.1016/S0896-6273(01)00245-8.

59. Gutiérrez, R. (2003). The GABAergic phenotype of the "glutamatergic" granule cells of the dentate gyrus. Prog. Neurobiol. *71*, 337–358. https://doi.org/10.1016/j.pneurobio.2003.11.004.

60. Boulanger, L.M., and Poo, M.M. (1999). Presynaptic depolarization facilitates neurotrophin-induced synaptic potentiation. Nat. Neurosci. *2*, 346–351. https://doi.org/10.1038/7258.

61. Ji, Y., Pang, P.T., Feng, L., and Lu, B. (2005). Cyclic AMP controls BDNF-induced TrkB phosphorylation and dendritic spine formation in mature hippocampal neurons. Nat. Neurosci. *8*, 164–172. https://doi.org/10.1038/nn1381.

62. Meyer-Franke, A., Wilkinson, G.A., Kruttgen, A., Hu, M., Munro, E., Hanson, M.G., Reichardt, L.F., and Barres, B.A. (1998). Depolarization and cAMP elevation rapidly recruit TrkB to the plasma membrane of CNS neurons. Neuron *21*, 681–693. https://doi.org/10.1016/S0896-6273(00)80586-3.

63. Jovanovic, J.N., Benfenati, F., Siow, Y.L., Sihra, T.S., Sanghera, J.S., Pelech, S.L., Greengard, P., and Czernik, A.J. (1996). Neurotrophins stimulate phosphorylation of synapsin I by MAP kinase and regulate synapsin I-actin interactions. Proc. Natl. Acad. Sci. USA *93*, 3679–3683. https://doi.org/10.1073/pnas.93.8.3679.

64. Tsien, J.Z., Huerta, P.T., and Tonegawa, S. (1996). The essential role of hippocampal CA1 NMDA receptor–dependent synaptic plasticity in spatial memory. Cell *87*, 1327–1338. https://doi.org/10.1016/S0092-8674(00)81827-9.

65. Leutgeb, J.K., Leutgeb, S., Moser, M.-B., and Moser, E.I. (2007). Pattern separation in the dentate gyrus and CA3 of the Hippocampus. Science *315*, 961–966. https://doi.org/10.1126/science.1135801.

66. Raam, T., McAvoy, K.M., Besnard, A., Veenema, A.H., and Sahay, A. (2017). Hippocampal oxytocin receptors are necessary for discrimination of social stimuli. Nat. Commun. *8*, 2001. https://doi.org/10.1038/s41467-017-02173-0.

67. Skogstrand, K., Hagen, C.M., Borbye-Lorenzen, N., Christiansen, M., Bybjerg-Grauholm, J., Bækvad-Hansen, M., Werge, T., Børglum, A., Mors, O., Nordentoft, M., et al. (2019). Reduced neonatal brain-derived neurotrophic factor is associated with autism spectrum disorders. Transl. Psychiatry *9*, 252. https://doi.org/10.1038/s41398-019-0587-2.

68. Pan, W., Banks, W.A., Fasold, M.B., Bluth, J., and Kastin, A.J. (1998). Transport of brain-derived neurotrophic factor across the blood–brain barrier. Neuropharmacology *37*, 1553–1561. https://doi.org/10.1016/S0028-3908(98)00141-5.

69. Caly, H., Rabiei, H., Coste-Mazeau, P., Hantz, S., Alain, S., Eyraud, J.-L., Chianea, T., Caly, C., Makowski, D., Hadjikhani, N., et al. (2021). Machine learning analysis of pregnancy data enables early identification of a subpopulation of newborns with ASD. Sci. Rep. *11*, 6877. https://doi.org/10.1038/s41598-021-86320-0.

70. Aguado, F., Carmona, M.A., Pozas, E., Aguiló, A., Martínez-Guijarro, F.J., Alcantara, S., Borrell, V., Yuste, R., Ibañez, C.F., and Soriano, E. (2003). BDNF regulates spontaneous correlated activity at early developmental stages by increasing synaptogenesis and expression of the K+/Cl- co-transporter KCC2. Development *130*, 1267–1280. https://doi.org/10.1242/dev.00351.

71. Uvarov, P., Ludwig, A., Markkanen, M., Rivera, C., and Airaksinen, M.S. (2006). Upregulation of the neuron-specific K+/Cl- cotransporter expression by transcription factor early growth response 4. J. Neurosci. *26*, 13463–13473. https://doi.org/10.1523/JNEUROSCI.4731-06.2006.

72. Ludwig, A., Uvarov, P., Soni, S., Thomas-Crusells, J., Airaksinen, M.S., and Rivera, C. (2011). Early growth response 4 mediates BDNF induction of potassium chloride cotransporter 2 transcription. J. Neurosci. *31*, 644–649. https://doi.org/10.1523/JNEUROSCI.2006-10.2011.

73. Szymanski, J., and Minichiello, L. (2022). NKCC1 deficiency in forming hippocampal circuits triggers neurodevelopmental disorder: role of BDNF-TrkB signalling. Brain Sci. *12*, 502. https://doi.org/10.3390/brainsci12040502.

74. Jonas, P., Major, G., and Sakmann, B. (1993). Quantal components of unitary EPSCs at the mossy fibre synapse on CA3 pyramidal cells of rat hippocampus. J. Physiol. *472*, 615–663. https://doi.org/10.1113/jphysiol.1993.sp019965.

75. Allen, C., and Stevens, C.F. (1994). An evaluation of causes for unreliability of synaptic transmission. Proc. Natl. Acad. Sci. USA *91*, 10380–10383. https://doi.org/10.1073/pnas.91.22.10380.

76. Tripathy, D., Vignoli, B., Ramesh, N., Polanco, M.J., Coutelier, M., Stephen, C.D., Canossa, M., Monin, M.-L., Aeschlimann, P., Turberville, S., et al. (2017). Mutations in TGM6 induce the unfolded protein response in SCA35. Hum. Mol. Genet. *26*, 3749–3762. https://doi.org/10.1093/hmg/ddx259.

77. Vignoli, B., Sansevero, G., Sasi, M., Rimondini, R., Blum, R., Bonaldo, V., Biasini, E., Santi, S., Berardi, N., Lu, B., and Canossa, M. (2021). Astrocytic microdomains from mouse cortex gain molecular control over long-term information storage and memory retention. Commun. Biol. *4*, 1152. https://doi.org/10.1038/s42003-021-02678-x.

STAR★METHODS

KEY RESOURCES TABLE

REAGENT or RESOURCE	SOURCE	IDENTIFIER
Antibodies		
Rabbit polyclonal α-phosphoTrkB (Tyr 816)	Provided by Moses Chao, Skirball Institute of Biomolecular Medicine, New York, USA.	N/A
Mouse α-PSD95	Merck -Millipore	Cat#MAB1596; RRID:AB_2092365
Chemicals, peptides, and recombinant proteins		
D-(−)-2-amino-5-phosphonopentaoic acid (D-AP5), 6,7-dinitroquinoxaline-2,3-dione (DNQX)	Tocris	Cat#0189/10
L-(+)-2-Amino-4-phosphonobutyric acid (L-AP4)	Tocris	Cat#0103/1
(2S,2′R,3′R)-2-(2′,3′-dicarboxycyclopropyl) glycine (DCG-IV)	Tocris	Cat#0975
Bicuculline	Tocris	Cat#0130/50
Picrotoxin	Tocris	Cat#1128
Gramicidin	SIGMA	Cat#G5002
Alexa Fluo 488	Life Technologies	Cat#A10436
BDNF	SIGMA	SRP3014
K252a	Merck (Calbiochem)	Cat#420298
DL-AP5	Tocris	Cat#0105
Experimental models: Organisms/strains		
NLG3^{R451C} knock-in mice: B6; 129-*Nlgn3*$^{tm2.1Sud}$/J	The Jackson Laboratory	RRID:IMSR_JAX:008,394
NLG3 knock-out mice	Prof. Peter Scheiffele, University of Basel	N/A
Software and algorithms		
pClamp	Molecular Devices	10.7
Prism	GraphPad	9.0
Nis- Element	Nikon	4.20.01

RESOURCE AVAILABILITY

Lead contact

Further information and requests for resources and reagents should be directed to and will be fulfilled by the lead contact, Enrico Cherubini (cher@sissa.it).

Materials availability

This study did not generate new unique reagents.

Data and code availability

- All data reported in this paper will be shared by the lead contacts upon request.
- This paper does not report original code.
- Any additional information required to re-analyze the data reported in this paper is available from the lead contacts upon request.

EXPERIMENTAL MODEL AND SUBJECT DETAILS

All experiments were performed in accordance with the Italian Animal Welfare legislation (D.L. 26/2014) that were implemented by the European Committee Council Directive (2010/63 EEC) and were approved by local veterinary authorities, the EBRI ethical committee and the Italian Ministry of Health (565/2018 PR).

$NLG3^{R451C}$ knock-in mice[10] were purchased from Jackson Laboratories (Maine, USA) whereas NLG3 knock-out mice were kindly provided by Prof. P. Scheiffele (University of Basel). Experiments were performed on off-spring male mice derived from heterozygous mating. We used only male mice because the *Nlg3* gene is localized on the X chromosome. Thus male carrying mutations/deletions are usually affected. Future investigations will determine whether also females carrying the mutation in heterozygous condition will show deficits in synaptic plasticity processes. Control experiments were performed on C57/B6 mice and on wild type littermates for $NLG3^{R451C}$ KI and NLG3 KO mice respectively.

Experiments and housing were in line with the ARRIVE guidelines. Mice were housed in 4–5 per cage, at constant temperature (22°C) and humidity (30–50%) and were kept on a regular circadian cycle (12 h:12 h light: dark cycle, lights on at 7:00 a.m.). Mice were provided with food and water *ad libitum*. All efforts were made to minimize animal suffering and to reduce the number of animals used.

METHOD DETAILS

Slice preparation

Hippocampal slices were obtained from neonatal (P2-P7) and juvenile (P18-P24) mice, using a standard protocol.[14] Animals were decapitated after being anesthetized with isoflurane (Sigma-Aldrich). The brain was rapidly removed from the skull and placed in a Petri dish filled with ice-cold cutting sucrose solution containing (in mM): 234 sucrose, 2.5 KCl, 1.25 NaH_2PO_4, 26 $NaHCO_3$, 10 $MgSO_4$, 0.5 $CaCl_2$, 11 glucose (saturated with 95% O_2 and 5% CO_2, pH 7.3-7.5). Transverse hippocampal slices (350-400 μm thick) were cut with a Leica vibratome (Leica VT12005) and stored at room temperature (20-24°C) in a holding bath containing the following (in mM): 130 NaCl, 3.5 KCl, 1.2 NaH_2PO_4, 27 NaHCO, 1.3 $MgCl_2$, 2 $CaCl_2$, 25 glucose (saturated with 95% O_2 and 5% CO_2, pH 7.3-7.5). After a recovery period of at least 1-h, an individual slice was transferred to the recording chamber where it was continuously superfused with oxygenated ACSF at a rate of 2-3 mL/min at 31-33°C.

Electrophysiological recordings

Electrophysiological experiments were performed on CA3 pyramidal cells using the whole-cell configuration of the patch-clamp technique in current or voltage-clamp mode. Neurons were visualized using an upright microscope (Nikon, Eclipse FN1) equipped with differential interference contrast (DIC) optics and infrared video camera. Patch electrodes were pulled from borosilicate glass capillaries (Hingelberg, Malsfeld). They had a resistance of 3-5 MΩ when filled with an intracellular solution containing (in mM): 140 KCl, 1 $MgCl_2$, 1 EGTA, 10 HEPES, 2 MgATP, (pH 7.3; 300-315 mOsm). Recordings were made with a patch clamp amplifier (Axopatch 200A, Molecular Devices). Hyperpolarizing pulses of 10 mV were routinely applied at 0.1 Hz to evaluate the passive properties of the membrane. Cells exhibiting more than 15-20% changes in series resistance were excluded from the analysis.

$GABA_A$-mediated postsynaptic potentials or currents (GPSPs or GPSCs) of mossy fibers (MF) origin were evoked at −70 mV in CA3 pyramidal neurons by stimulation of granule cells in the dentate gyrus (at 0.05 Hz) using concentric bipolar electrodes in the presence of DNQX (20 μM) and D-AP5 (50 μM) to block AMPA- and NMDA mediated synaptic responses, respectively. We used minimal stimulation of the granule cells in order to activate only one or few presynaptic fibers. According to the technique described by Jonas et al. (1993) and Allen and Stevens (1994),[74,75] the stimulation intensity was decreased until only a single axon was activated. This was achieved when the mean amplitude of the postsynaptic currents and failure probability remained constant over a range of stimulus intensities near threshold for detecting a response.[40] An abrupt increase in the mean peak amplitude of synaptic currents was observed when the stimulus intensity was further increased. This all or none behavior let us to assume that only a single fiber was stimulated. In addition, the latency and the shape of individual synaptic responses remained constant for repeated stimuli.

MF-GPSCs were identified on the basis of their sensitivity to group III mGluR agonist 2-amino-4-phosphonobutyric acid (L-AP4, 10 μM), their strong paired-pulse facilitation and short term frequency-dependent facilitation.[40] MF-GPSCs were blocked by bicuculline (10 μM) or picrotoxin (100 μM), confirming their GABAergic nature. In contrast to MF inputs, GABAergic inputs from interneurons were insensitive to L-AP4.[40]

In juvenile mice excitatory postsynaptic potentials or currents (EPSPs-EPSCs) of MF origin were recorded in CA3 principal cells following stimulation of MF in *stratum lucidum*, in the presence of picrotoxin (100 μM) to block $GABA_A$-mediated synaptic inhibition. MF-EPSCs were identified on the basis of their pronounced paired-pulse ratio (PPR) and their sensitivity to group II mGluR agonist DCG-IV (1 μM).

Synaptic currents were recorded in voltage clamp mode for at least 10 min. Then, changes in synaptic efficacy were induced by applying a pairing protocol in current clamp conditions: MF stimulation with post-synaptic spiking (in neonates: 10 spikes at 0.1 Hz, 15 ms after MF stimulation; in juveniles 50 spikes at 0.1 Hz, 10 ms after MF stimulation). After pairing, MF GPSCs were recorded in voltage clamp conditions for an additional 30-40 min. STD-LTP was usually induced in neurons loaded via the patch pipette with Alexa Fluor 488 dye (Thermo Fisher Scientific). This allowed to unveil possible changes in BDNF/TrkB signaling pathway using post-hoc immuno-labelling and high-resolution microscopy in neurons exposed to the pairing protocol.

Gramicidin-perforated patch recordings

GABA-mediated postsynaptic currents (GPSCs) evoked in CA3 principal cells by stimulation of MFs in *stratum lucidum* (in the presence of DNQX and DL-AP5 to block NMDA and AMPA receptors, respectively) were recorded (from a holding potential of −70 mV) using gramicidin perforated patch. In this case, the patch pipette solution contained (in mM): 150 KCl and 10 HEPES, buffered to pH7.2 with Tris-OH. The extracellular solution contained (in mM): NaCl 130, KCl 3.5, NaH_2PO_4 1.2, $NaHCO_3$ 25, $MgCl_2$ 1.3, $CaCl_2$ 2, glucose 25, saturated with 95% O2 and 5% CO2 (pH 7.3-7.4). Gramicidin was first dissolved in DMSO to prepare a stock solution of 10–40 mg/mL and then diluted in the pipette solution to a final concentration of 80 μg/mL. The gramicidin-containing solution was prepared and sonicated <1 h before the experiment. To facilitate cell-attached formation (4–10 GΩ), patch pipettes were backfilled with a gramicidin-containing solution. Recordings started 20-30 min after formation of the cell-attached seal and stabilization of the series resistance (*Rs*) around 60 MΩ. Depolarizing currents were intermittently injected to evoke action potentials to verify the patch integrity, and in the case of membrane rupture, the recording was discontinued. At the end of each recording, negative pressure was applied to break the membrane and establish whole-cell configuration. This was associated with a shift of the reversal potential of the GABA-mediated responses to near 0 mV.

Drugs

Drugs used were: D-(−)-2-amino-5-phosphonopentaoic acid (D-AP5), 6,7-dinitroquinoxaline-2,3-dione (DNQX), L-(+)-2-Amino-4-phosphonobutyric acid (L-AP4), (2S,2′R,3′R)-2-(2′,3′-dicarboxycyclopropyl) glycine (DCG-IV), DL-AP5, bicuculline, picrotoxin (PTX, all purchased from Tocris Cookson Ltd, Bristol, UK), Brain Derived Neurotrophic Factor (BDNF) (Sigma-Aldrich) K252a (Sigma-Aldrich).

All drugs were dissolved in either distilled water or ethanol, as required, except DNQX that was dissolved in dimethylsulphoxide (DMSO). The final concentration of DMSO in the bathing solution was 0.1%. At this concentration, DMSO alone did not modify the shape or the kinetics of synaptic currents. Drugs were applied in the bath via a three-way tap system, by changing the superfusion solution to one differing only in its content of drug(s). The ratio of flow rate to bathe volume ensured complete exchange within 1-2 min.

Electrophysiology data acquisition and analysis

Data were acquired at 20 kHz, filtered with a cut-off frequency of 2 kHz and stored on a computer in order to perform offline analysis. MF GPSC and GPSPs were analyzed using pClamp 10.0 (Molecular Devices, Sunnyvale, CA, USA). Mean MF GPSCs amplitude was obtained by averaging successes and failures. The paired pulse ratio (PPR) was calculated as the mean amplitude of the synaptic response evoked by the second stimulus over that evoked by the first one (at 50 ms interval). The coefficient of variation was calculated as the ratio between the SD of synaptic currents amplitude and the mean.

Immunohistochemistry

Brain slices were fixed in 4% PFA for 2 h after recording. Slices were treated with 1% Triton X-100 for 20 min, blocked with 3% BSA in PBS for 1 h and incubated overnight free-floating with primary antibodies diluted in blocking buffer. Slices were washed in PBS and incubated for 2 h at room temperature with secondary antibodies diluted in blocking buffer. Slices were counterstained with DAPI and mounted with Aqua Polymount (Polyscience Inc.).[76,77]

Antibodies

The following antibodies were used: rabbit α-pTrkB (Tyr 816) (provided by Moses Chao, Skirball Institute of Biomolecular Medicine, New York, USA, IHC 1.25 μg/mL); mouse α-PSD95 (Merck -Millipore, Cat#MAB1596, IHC 1:500). Alexa fluorochrome conjugated secondary antibodies were purchased from Jackson Immunoresearch.

Confocal microscopy and quantitative image analysis

Confocal imaging was performed using a laser-scanning motorized confocal system (Nikon A1) equipped with an Eclipse Ti-E inverted microscope and four laser lines (405, 488, 561 and 638 nm). z series images were taken with an inter-stack interval of 0.5 μm using 60× oil objective. Image processing were performed using the software NIS Element (Nikon, Japan). The co-localization signal of PSD95 and Alexa 488 was obtained using the software NIS Element (Nikon, Japan). Co-localization signal was superimposed to pTrkB signal and the number of PSD95/Alexa 488 spines expressing pTrkB were manually counted in single stack images and expressed as a percentage of the total number of PSD95/Alexa 488 spines. CA3 principal cells subjected to STDP were stimulated by the protocol described in "electrophysiological recording" section, while cells classified as "no pairing" were stimulated without pairing MF stimulation with postsynaptic spikes.

3D- structured illumination microscopy

3D- SIM was performed using an X-light V2 confocal spinning disk system completed with a Video Confocal super-resolution module (CrestOptics, Italy) with a lateral resolution of 115 nm and an axial resolution of around 250 nm. The system was equipped with 60X/1.40NA PlanApo Lamda oil immersion objective (Nikon, Japan), Zyla sCMOS camera (Andor) and Spectra X Lumencor LEDs Light source with bandpass excitation filters of 460-490 nm and 535-600 nm (Chroma Technology, US). Image stacks were acquired with a format of 2048 X 2048 pixels and a z distance of 150 nm and with 36 raw images per plane (multiple acquisition mode x-y grid scan). The SIM raw data with 16-bit depth were computationally reconstructed using the Metamorph software package. The triple co-localization was performed in two steps: the binary signal representing the co-localization between Alexa and PSD95 was over posed on the binary signal obtained by the co-localization of PSD95 and pTrkB signals. The logical function "AND" was applied to both binary signals to highlight the presence of three different signals. 3D-image rendering, and co-localization analysis were performed using Nis-Elements software (Nikon, Japan).

QUANTIFICATION AND STATISTICAL ANALYSIS

All values are presented as mean ± SEM Statistical comparisons were performed using a *t*-test or a non-parametric test, depending on whether data were normally distributed or not. Details on the number of cells, the type of statistical test used and on significance of the data are provided in the figure legends. A p value <0.05 was considered as statistically significant.